JCI insight

Impact of mechanical unloading on genome-wide DNA methylation profile of the failing human heart

Xianghai Liao, … , Gordana Vunjak-Novakovic, Veli K. Topkara

JCI Insight. 2023. https://doi.org/10.1172/jci.insight.161788.

Research In-Press Preview Cardiology

Graphical abstract

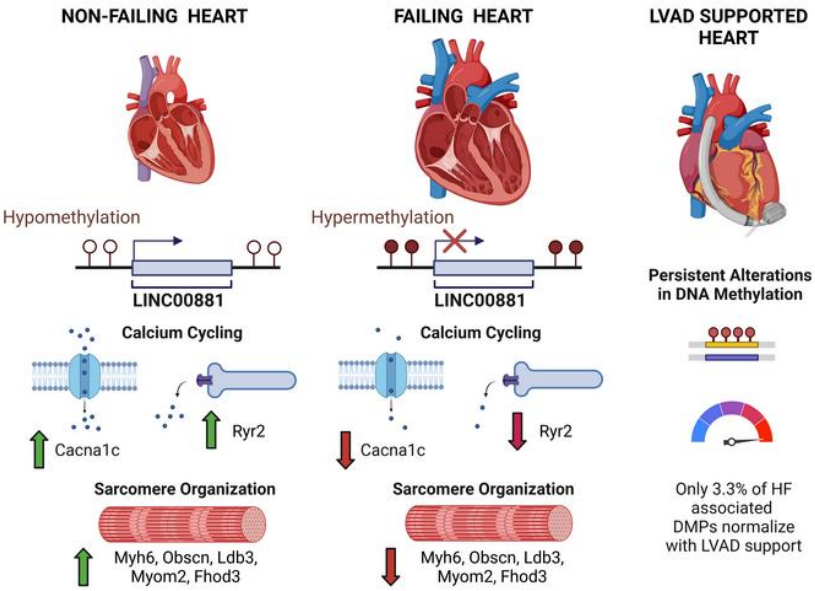

Impact of Mechanical Unloading on Genome-Wide DNA Methylation Profile of the Failing Human Heart

Xianghai Liao, PhD[1*], Peter J. Kennel, MD[1*], Bohao Liu, MD, PhD[2], Trevor R. Nash, PhD[2], Richard Z. Zhuang, PhD[2], Amandine F. Godier-Furnemont, MD PhD[2], Chenyi Xue, MSc[1], Rong Lu, BS[1], Paolo C. Colombo, MD[1], Nir Uriel, MD[1], Muredach P. Reilly, MD[1], Steven O. Marx, MD[1], Gordana Vunjak-Novakovic, PhD[2], Veli K. Topkara, MD MSc[1].

[1] Division of Cardiology, Columbia University Irving Medical Center – New York Presbyterian, New York, NY
[2] Department of Biomedical Engineering, Columbia University, New York, NY

Authorship Note: *XL and PJK contributed equally to this work

Brief Title: Genome-wide DNA Methylation in Human Heart Failure

Key words: Heart failure; Epigenetics; Non-coding RNA

Word count: 8,819

Sources of Funding: V.K.T. is supported by NIH (HL146964). G.V.N is supported by grants from the NIH (UH3EB025765, P41EB027062, and R01HL076485) and NSF (NSF16478). This research was supported by the Lisa and Mark Schwartz Program to Reverse Heart Failure at New York–Presbyterian Hospital/Columbia University.

Disclosures: None

Corresponding Author:
Veli K. Topkara, M.D., M.Sc.
Assistant Professor of Medicine
Center for Advanced Cardiac Care
Columbia University Medical Center – New York Presbyterian
622 West 168th St, PH10-203A
Phone: (212) 305-4600
Fax: (212) 305-7439
Email: vt2113@cumc.columbia.edu

Abstract

Heart failure (HF) is characterized by global alterations in myocardial DNA methylation, yet little is known about epigenetic regulation of the non-coding genome and potential reversibility of DNA methylation with left ventricular assist device (LVAD) therapy. Genome-wide mapping of myocardial DNA methylation in 36 HF patients at LVAD implantation, 8 patients at LVAD explantation, and 7 non-failing donors using a high-density bead array platform identified 2079 differentially methylated positions (DMPs) in ischemic cardiomyopathy and 261 DMPs in non-ischemic cardiomyopathy. LVAD support resulted in normalization of 3.2% of HF-associated DMPs. Methylation-expression correlation analysis yielded several protein-coding genes that are hypomethylated and upregulated (*HTRA1*, *FBXO16*, *EFCAB13*, *AKAP13*) or hypermethylated and downregulated (*TBX3*) in HF. A novel cardiac-specific super-enhancer lncRNA (*LINC00881*) is hypermethylated and downregulated in human HF. *LINC00881* is an upstream regulator of sarcomere and calcium channel gene expression including *MYH6*, *CACNA1C*, and *RYR2*. *LINC00881* knockdown reduces peak calcium amplitude in the beating human iPS cell derived cardiomyocytes. Collectively, these data suggest that HF-associated changes in myocardial DNA methylation within coding and non-coding genome are minimally reversible with mechanical unloading. Epigenetic reprogramming strategies may be necessary to achieve sustained clinical recovery from heart failure.

Introduction

Heart failure (HF) is a major public health problem with more than 6 million patients affected in the United States alone.(1) Despite significant progress achieved in the diagnosis and treatment of HF, the majority of patients progress to advanced stages of the disease leading to unacceptably high rates of morbidity and mortality, even exceeding most cancers. Pharmacological management of HF has traditionally focused on targeting endogenous neurohormonal signaling cascades that are associated with disease progression as well as diuretic therapy for symptom relief.(2) Yet, our limited mechanistic understanding of the complex HF pathophysiology does not fully explain the wide variation in disease progression and treatment response observed in this population, highlighting the need for novel molecular diagnostic and therapeutic strategies.

The failing human heart undergoes structural and functional remodeling that is accompanied by profound alterations in the myocardial transcriptome including recapitulation of the fetal gene expression program and downregulation of the genes involved in the oxidative phosphorylation pathway.(3, 4) While some of these changes are common to all forms of heart failure, gene expression could be etiology-specific and help distinguish patients with different types of HF.(5, 6) Transcriptional profiling of paired myocardial samples obtained from patients with advanced HF before and after left ventricular assist device (LVAD) support demonstrate that only a small percentage of genes that are dysregulated in HF normalize with mechanical unloading of the failing human heart.(7-9) While the mechanisms responsible for the persistent dysregulation of myocardial gene expression in the end-stage human HF remains unknown, emerging evidence suggest that epigenetic regulation may play important roles in transcriptional reprogramming by altering gene accessibility and TF binding to gene promoters or enhancers.(10, 11)

DNA methylation is an essential epigenetic modification involving transfer of a methyl group onto the fifth position of the cytosine catalyzed by a family of DNA methyltransferases (DNMTs) and generally signals for transcription repression at the promoter sites.(12) Several pathological conditions, in particular malignant transformation, have been associated with hyper-methylation of specific target gene promoters as well as global hypomethylation leading to genomic instability.(13) DNA methylation assays have been FDA approved for early detection of cancer and DNA demethylation agents have become standard of care therapy for high-risk patients with myelodysplastic syndrome.(14-16) While the data is lagging for HF, several studies to date investigated genome-wide DNA methylation in the failing human heart using targeted bisulphite sequencing or chip-based approaches.(17-23) However, none of these studies have examined whether or not, and if so to what extent aberrant DNA methylation is reversible in the failing human heart. Moreover, HF-associated changes in DNA methylation of non-coding genomic elements including long non-coding RNAs (lncRNAs) remain largely unknown. Hence, in the current study we characterize myocardial DNA methylation profile of patients with end-stage cardiomyopathy before and after mechanical unloading with left ventricular assist device (LVAD) support. Furthermore, we identify a novel cardiac-specific and super-enhancer associated long-noncoding RNA (*LINC00881*), that is hypermethylated and downregulated in the failing human heart, as a key regulator of calcium handling in the cardiomyocyte.

Results

Myocardial DNA Methylation in Ischemic and Non-Ischemic Cardiomyopathy

36 patients with end-stage heart failure (12 Ischemic [ICM] and 24 Non-Ischemic [NICM] dilated cardiomyopathy) who underwent LVAD implantation at Columbia University Irving Medical Center and 7 non-failing controls were included for genome-wide DNA methylation

analysis. Analysis pipeline has been summarized in **Supplemental Figure 1**. Patients with myocarditis, amyloid cardiomyopathy, restrictive/hypertrophic cardiomyopathy, and previous cardiac transplantation were excluded from the study. Demographics and clinical characteristics of HF patients with myocardial genome-wide DNA methylation profiling at the time of LVAD implantation was summarized in **Table 1**. Paired post-LVAD cardiac samples were obtained from 8 patients who were bridged to heart transplantation. LVAD support resulted in significant reductions in left ventricular end-diastolic diameter, and a trend towards increased LVEF and decreased serum BNP levels in 8 patients (**Supplemental Table 1A**). Clinical information of non-failing cardiac donors has been provided in **Supplemental Table 1B**. Histopathological examination of human heart tissue samples demonstrated cardiomyocyte hypertrophy and myocardial fibrosis in pre-LVAD patients compared to non-failing controls consistent with HF phenotype (**Figure 1A**). Cardiomyocyte hypertrophy significantly regressed with LVAD support while myocardial fibrosis did not. qPCR analysis demonstrated upregulation of *NPPA, MYH7,* and *COL1A1* genes in HF compared to non-failing controls. LVAD support resulted in significant downregulation of *NPPA* and *MYH7* genes but not *COL1A1* gene (**Figure 1B**).

Genome-wide DNA methylation profiling identified 2079 differentially methylated positions (DMPs) in myocardium of patients with ischemic cardiomyopathy (ICM vs. NF, $q < 0.05$, **Supplemental Table 2**). Of those 625 DMPs were hypermethylated and 1454 DMPs were hypomethylated. 261 DMPs were differentially methylated in myocardium of patients with non-ischemic cardiomyopathy (NICM vs. NF, $q < 0.05$, **Supplemental Table 3**). Of those, 117 DMPs were hypermethylated and 144 DMPs were hypomethylated in NICM. 192 DMPs (**Supplemental Table 4**) were common to both ICM and NICM patients (**Figure 2A**). All of these "common HF

DMPs" were either concordantly hypomethylated (n=125) or concordantly hypermethylated (n=67) in ICM and NICM.

Characterizing the location of DMPs within gene regions, for ICM and NICM similarly, higher proportion of probes located within transcription start site were hypermethylated than hypomethylated, whereas intergenic region probes were more likely to be hypomethylated than hypermethylated (**Figure 2B**). DMPs within open sea regions were more likely to be hypomethylated whereas DMPs within CpG islands and associated shores were more likely to be hypermethylated in both ICM and NICM (**Figure 2B**). 17.9% of DMPs mapped to promoter regions (TSS200, TSS1500, and 5'UTR) in ICM patients compared to 22.2% of DMPs in NICM patients. Principal component analysis (PCA) of genome-wide methylation levels demonstrates clustering of the non-failing versus failing samples, however, did not clearly separate between subjects with ischemic vs non-ischemic etiology (**Figure 2C**). Heatmap of methylation level Z-scores of 192 common HF DMPs across non-failing healthy controls and HF samples with unbiased hierarchical heatmap clustering separated the non-failing controls from the failing heart DMPs but did not separate ICM from NICM (**Figure 2D**).

Minimal Reversibility of Myocardial DNA Methylation with LVAD Support

Patterns of myocardial DNA methylation were analyzed in paired myocardial samples obtained from 8 patients before and after LVAD support. 1075 CpG sites were differentially methylated in the failing myocardium compared to non-failing (pre-LVAD vs NF, $q < 0.05$, **Supplemental Table 5**). In contrast, only 130 CpG sites were differentially methylated with LVAD support (post-LVAD vs. pre-LVAD, $q<0.05$, **Supplemental Table 6**). Only 35 CpG sites (**Supplemental Table 7**) were common in heart failure and reverse remodeling (**Figure 3A**), all of which were methylated in opposite direction.

Higher proportion of DMPs located within gene bodies and transcription start sites were hypermethylated while DMPs located within intergenic regions (IGR) were hypomethylated in HF. Conversely, higher proportion of probes located within gene bodies and transcription start sites were hypomethylated while DMPs located within intergenic regions (IGR) were hypermethylated in Reverse Remodeling (RR), suggesting an opposite trend between HF and RR (**Figure 3B**). PCA of genome-wide methylation levels demonstrated clustering of the non-failing versus pre-LVAD samples, but not pre-vs post-VAD samples, suggesting only minor changes in global DNA methylation with mechanical unloading (**Figure 3C**). Heatmap of methylation level Z-scores of 35 LVAD-responsive HF DMPs across non-failing and paired LVAD samples with unbiased hierarchical clustering demonstrated grouping of post-LVAD samples with 8 out of 9 non-failing control samples (**Figure 3D**), confirming LVAD-induced changes in DNA methylation towards non-failing state in these genomic positions.

Integrated Analysis of DNA Methylation with Gene Expression in the Failing Human Heart

The classical paradigm of promoter DNA methylation as a transcriptional silencing mechanism has recently been challenged with growing lines of evidence suggesting that DNA hypermethylation could also result in transcriptional activation.(24-26) Accordingly, we assessed the relationship between differentially methylated CpG sites and changes in gene expression levels using a large publicly available transcriptional dataset obtained from heart failure patients.(5) Out of 192 common HF DMPs, 121 CpG sites map to 93 protein-coding genes (**Figure 4A**). Out of those, 74 genes were expressed in the myocardium (RPKM >1), and 34 were differentially expressed in human heart failure. When changes in DNA methylation were correlated with the changes in gene expression, 14 genes were hypomethylated and transcriptionally upregulated, 13 genes were hypomethylated and transcriptionally downregulated, 6 genes were hypermethylated

and transcriptionally upregulated, and 1 gene was hypermethylated and transcriptionally downregulated (**Table 2**). Using independent cardiac tissue samples obtained from patients with end-stage ICM and NICM, we validated upregulation of *AKAP13* (fold change [FC] = 2.98), *HTRA1* (FC= 1.52), *EFCAB13* (FC= 2.86), and *FBXO16* (FC= 1.92) as well as downregulation of *TBX3* (FC= 0.39) in the failing human hearts by qPCR analysis, while changes in *RPTOR* and *HDAC9* transcripts did not reach statistical significance (**Figure 4C**).

Super-enhancer region associated LINC00881 is downregulated in the Failing Human Heart

Common HF and LVAD responsive HF DMPs located in intergenic regions were screened for the presence of overlapping non-coding RNAs using GENCODE and NONCODE datasets. We identified a novel long intergenic non-protein coding RNA (*LINC00881*) located~9 kb upstream of a significantly hypermethylated CpG site (cg01535205) (**Supplemental Table 8**). *LINC00881* is highly and exclusively expressed in human myocardium according to GTEx, which made it an interesting candidate for further exploration in the context of epigenetic modification of the failing heart (**Supplemental Figure 2**). Interestingly, *LINC00881* and cg01535205 are located within a cardiac super-enhancer region (**Supplemental Figure 3**). RNA-seq and CHIP-seq tracks confirms high expression of *LINC00881* in the adult non-failing human heart as well as presence of active chromatin marks in this region including H3K27ac (**Figure 5A**). qPCR of *LINC00881* in independent HF samples confirmed that this intergenic RNA is downregulated in ICM and NICM compared to myocardium from healthy controls (**Figure 5B**). *LINC00881* is largely restricted to the nuclear compartment as opposed to cytoplasmic in human induced pluripotent stem-cell derived cardiomyocytes (hiPSC-CMs) (**Figure 5C**). Inhibition of DNA methyltransferase using 5-Azacytidine (5-AZA) resulted in significant upregulation of *LINC00881* transcript levels in the beating hiPSC-CMs, suggesting epigenetic regulation of *LINC00881* in

cardiomyocytes (**Figure 5C**). *LINC00881* expression was significantly upregulated during differentiation of hiPSC-CMs, in parallel with upregulation of transcription factors including *GATA4*, *HAND2*, and *TBX5*, confirming its role as a cardiomyocyte lineage specific super-enhancer lncRNA (**Figure 5D**).

To explore the mechanistic basis of *LINC00881* dysregulation in human heart failure, we used plasmid-mediated overexpression and GapmeR-based knockdown of *LINC00881* in the beating hiPSC-CMs (**Supplemental Figures 4 and 5)**. RNA-sequencing identified 1545 genes that were differentially expressed with *LINC00881* overexpression (**Supplemental Table 9**) and 2268 genes that were differentially expressed with *LINC00881* knockdown (p-value cut-off <0.05) (**Supplemental Table 10**). Among 199 common genes that were differentially regulated in both *LINC00881* overexpression and *LINC00881* knockdown models, 174 (87.4%) were regulated in opposite directions including 73 genes that are positively regulated and 101 genes that are negatively regulated by *LINC00881* (**Figure 6A** and **Supplemental Table 11**). Gene Ontology analysis of gene targets that are positively regulated by *LINC00881* were enriched in sarcomere organization (*MYH6, OBSCN, LDB3, MYOM2, FHOD3),* calcium ion transport (*CACNA1C, CACNA1D, RYR2, CAMK2A, ANXA6),* ventricular tissue morphogenesis *(FGFR2, MYH6, TNNI1),* and fatty acid beta-oxidation (*MECR, ACAD10, PPARD*) pathways (**Figure 6B)**. Gene Ontology analysis of gene targets that are negatively regulated by *LINC00881* were enriched in transcription from RNA II polymerase promoter (*CEBPG*, *KLF5*, *KLF10*, *SMAD5*, *ATF1*, *ATF3*, and *ANKRD1)* and regulation of apoptotic process (*BCLAF1, DNAJA1, GNA13, MCL1, ANRKRD1, PHLDA1, SIRT1*) pathways. *LINC00881* regulation of select sarcomere and calcium channel target genes were validated in hiPSC-CMs by qPCR with or without *LINC00881* knockdown (**Figure 6C**). To determine whether *LINC00881* regulation of sarcomere and calcium

channel genes have functional relevance in the heart, we measured calcium transients in beating hiPSC-CMs treated with GapmeRs targeting *LINC00881* versus scrambled control oligonucleotide. *LINC00881* knockdown resulted in significant reductions in the peak calcium amplitude in hiPSC-CMs (**Figure 6D**).

To gain further insights into *LINC00881* regulation of cardiomyocyte gene expression, we performed in-silico target prediction analysis using RNAct database and identified 54 putative *LINC00881* interacting proteins (**Supplemental Table 12**). Candidate *LINC00881* targets were significantly enriched for chromatin remodeling pathway proteins including *BICRA, CECR2, ERCC6, SMARCA2, SMARCA4, BAZ1A, BAZ1B,* and *RSF1* (**Figure 7A)**. RNA-seq analysis in hiPSC-CMs suggested borderline significance for differential regulation of *SMARCA4* by *LINC00881* overexpression and knockdown, but not the other putative targets. *LINC00881* regulation of *SMARCA4* was validated in hiPSC-CMs by RT-qPCR (**Figure 7B)**. In vitro RNA immunoprecipitation in hiPSC-CMs showed that *LINC00881* but not *GAPDH* was co-precipitated by *SMARCA4* **(Figure 7C)**. Chromatin accessibility experiment in hiPSC-CMs demonstrated a significant increase in *RYR2* promoter accessibility with *LINC00881* overexpression in hiPSC-CMs (**Figure 7D**).

Discussion

The present study utilized bead array technology for high-density genome-wide mapping of DNA methylation in the failing human heart before and after LVAD support. Our analysis identified myocardial DNA methylation patterns that are associated with reciprocal regulation of gene expression in patients with ICM and NICM. In addition to providing the most comprehensive mapping of etiology-specific changes in myocardial DNA methylation to date, we show for the first time that mechanical unloading with LVAD is associated with an incomplete normalization

of the myocardial DNA methylation profile, suggesting that HF-related epigenetic alterations could be persistent. Moreover, our analysis identified a novel cardiac-specific super-enhancer lncRNA gene (*LINC00881*), which is hypermethylated and downregulated in the failing human heart, as an essential regulator of cardiomyocyte calcium cycling.

DNA Methylation in Human Heart Failure

Consistent with previous reports, we found that the majority of differentially methylated positions in end-stage human heart failure had reduction in DNA methylation levels, suggesting a global hypomethylation similar to what has been demonstrated in cancer biology.(17, 18, 20, 27) Movassagh et al. demonstrated that HF-related differential methylation in CpG islands was predominantly located in gene promoters and gene bodies, but not in intergenic or 3'UTRs.(17) Our analysis expands on this observation and demonstrates a large number of intergenic positions that are also differentially methylated, including a subset mapping to non-coding genome. Our etiology-specific analysis identified 192 DMPs that were common to patients with ICM (2079 DMPs) and NICM (261 DMPs), similar to a recent study by Glezeva et al. which identified 13 common HF DMPs from patients with ICM (51 DMPs) and NICM (118 DMPs).(20) Overlapping DNA methylation profiles in patients with ICM and NICM support a convergent "final common pathway" of gene expression that are found in all forms of heart failure irrespective of the inciting event. Our analysis showed that hypomethylated CpG sites, particularly in ICM, were more likely to be within gene body or intergenic regions as opposed to transcription start sites, which is consistent with a prior study by Pepin et al. demonstrating a relative hypermethylation of promoter-associated CGIs in ICM patients.(28) 25 out of 93 common HF DMPs mapping to a protein-coding gene in current study were also found to be differentially methylated in at least one previous study validating our analytical approach.(18, 22, 23) Interestingly, we did not find differential DNA

methylation for HF marker genes with the exception of *NPPB* promoter, which was significantly hypomethylated in NICM and ICM samples with a delta-beta value below the detection cut-off level of 10%. Hypomethylation of natriuretic peptide gene promoters in HF patients has been previously demonstrated by some(22, 23), but not all genome-wide DNA methylation studies(17, 18, 20). A plausible explanation for this discrepancy is that most studies to date used whole myocardium for DNA methylation profiling which could dilute cardiomyocyte-specific epigenetic signals. It is also possible that alternative epigenetic modifications such as histone modification may play a role in transcriptional regulation of HF marker genes.(29)

Effect of Mechanical Unloading with LVAD on Myocardial DNA Methylation Patterns

Mechanical unloading with LVAD is associated with favorable changes in the biology of the failing cardiomyocyte including regression of myocyte hypertrophy, improvement in excitation-contraction coupling, and down-regulation of the fetal gene expression, also termed as reverse remodeling, which results in normalization of cardiac function in a small number of patients allowing for LVAD explantation.(30-33) Transcriptional studies of paired myocardial samples obtained from patients with end-stage heart failure before and after LVAD support demonstrate that only <5% of HF-related transcripts normalize with LVAD support.(7, 9) Consistent with these observations, we found that only 3.2% of HF-related DMPs were reverse methylated with LVAD support, which may in part explain persistent transcriptional dysregulation and the low incidence of myocardial recovery in patients supported by LVAD. Since DNA methylation is a reversible phenomenon, these findings raise the possibility that epigenetic modulation may be necessary to normalize the HF transcriptome and achieve myocardial recovery. In support of this hypothesis, inhibition of DNA methylation using 5-aza-2′-deoxycytidine rescued a HF phenotype in a rat model of norepinephrine induced cardiac hypertrophy.(34) Mice with

cardiomyocyte-specific deletion of *Dnmt3b* develop cardiomyopathy with sarcomeric disarray and interstitial fibrosis.(35) Similarly, differences in myocardial DNA methylation among mouse strains has been shown to determine susceptibility to cardiac hypertrophy following isoproterenol treatment.(36) Taken together, these findings suggest that epigenetic reprogramming may have therapeutic relevance in heart failure and additional research is necessary to elucidate the mechanistic basis of this approach.

Common Heart Failure DMPs with Reciprocal Changes in Gene Expression

Our analysis identified a subset of differentially methylated protein-coding genes, which were transcriptionally regulated in the opposite direction of methylation in HF. Among upregulated genes were *HTRA1*, *FAM65B*, *UNC45A*, *KALRN*, *AKAP13*, *RPTOR*, and *HDAC9*, which have been previously implicated in maladaptive hypertrophy. *HTRA1* has been identified as part of a candidate gene signature correlated with cardiomyopathies in a gene correlation network analysis model and its mRNA expression is upregulated 6.9 fold in DCM.(37, 38) *PINK1* dependent phosphorylation of *FAM65B* attenuates ischemia reperfusion injury by suppressing autophagy.(39) The *UNC45A* gene has been characterized as potential de novo mosaic variant in sporadic cardiomyopathy.(40) *KLRN* is a Rho Guanine Nucleotide Exchange Factor (*GEF*), which is downregulated in ICM and NICM hearts.(41) A-Kinase Anchoring Protein 13 (*AKAP13*) promotes downstream hypertrophic gene expression, mediated at least in part via *HDAC5* phosphorylation and *MEF2*-mediated transcription in TAC model of cardiac hypertrophy.(42) Genetic deficiency of *RPTOR*, regulatory associated protein of mTOR Complex 1, leads to reduction of mTORC1 activity and dilated cardiomyopathy in mice.(43) Mice lacking *HDAC9* are sensitized to hypertrophic signals and exhibit stress-dependent cardiomegaly.(44) *miR-21* levels

are increased selectively in fibroblasts of the failing heart.(45) In vivo silencing of *miR-21* has been shown to attenuate cardiac dysfunction.(45, 46)

TBX3 was the only protein-coding gene common to ICM and NICM with DNA hypermethylation and transcriptional downregulation in our analysis. *TBX3* is located within the 12q24.21 locus, which harbors several other genes that have previously been linked to cardiomyopathies. Meder et al. identified this gene locus to be differentially methylated in NICM patients, validating our observation.(23) Genetic variation in *TBX3* was associated with LV mass in health Japanese population, highlighting potential implication in cardiac hypertrophy, however precise mechanisms warrants further investigation.(47) In addition, we identified and validated several genes that were hypomethylated and upregulated in the failing human heart with previously unknown link to HF including *FXBO16*, *EFCAB13*, *COL18A1*, *PLXNA2*, *BRE*, *KIAA0922*, and *MAP3K14*. Additional research is warranted to investigate the function of these genes in the HF pathophysiology.

Role of LINC00881 in Human Heart Failure

Our genome-wide screening identified a novel lincRNA with epigenetic and transcriptional dysregulation in human heart failure. *LINC00881* is transcribed from a cardiac specific super-enhancer region with abundant expression levels in the adult human heart. We show that this super-enhancer region is hypermethylated which is associated with down-regulation of *LINC00881* gene expression in patients with ICM and NICM. In cardiomyocytes, DNA demethylation treatment also resulted in upregulation of *LINC00881* transcript levels. To date, very little has been known regarding the role and function of *LINC00881* except that it is expressed in cardiomyocytes and regulated by a *GATA4* responsive super-enhancer element.(48, 49) *LINC00881* (NR_034008) was listed among significantly down-regulated transcripts in the failing human heart in two

independent transcriptomic publications validating our observation.(5, 50) Our in-vitro work in beating hiPSC-CMs expands on the role of LINC00881 in human HF and suggest that it is an essential regulator of cardiomyocyte calcium cycling and an upstream transcriptional regulator of several key calcium channel and sarcomere organization genes including *CACNA1C*, *RYR2*, and *MYH6*. In silico target prediction and chromatin accessibility data suggest that transcriptional regulation of *LINC00881* target genes is in part mediated by chromatin remodeling, which is a common mechanism for lncRNAs that are localized in nucleus. Furthermore, we identify *SMARCA4* as a *LINC00881* interacting protein in hiPSC-CMs. *SMARCA4* belongs to ATP-dependent chromatin remodeling complex SWI/SNF and plays critical roles during cardiac differentiation and development.(51, 52) Initial studies in mice have demonstrated that *Smarca4* is turned off in adult cardiomyocytes and reactivated upon cardiac stress to regulate myosin heavy chain isoform switching as a maladaptive response.(53) Emerging data however indicate that depletion of *Smarca4* levels in post-natal cardiomyocytes by adenoviral-based siRNA knockdown or dual genetic knockout strategy with *Smarca2* causes lethal cardiomyopathy in mice.(54, 55) Furthermore, single-cell transcriptome profiling from the normal adult human heart demonstrated that *SMARCA4* was highly expressed in human atrioventricular cardiomyocytes.(56) Expression of *SMARCA4* and its occupancy at target gene promoters were significantly decreased in human heart failure(55, 57), suggesting distinct roles for this chromatin remodeler in the adult human heart under basal and stress conditions.

Limitations of the study include unknown confounders that may influence DNA methylation patterns in the human myocardium. Cardiac tissue is composed of multitude of cell types including cardiomyocytes, fibroblasts, endothelial cells, and immune cells, which likely have distinct methylation profiles. Since our study utilized myocardial DNA for profiling, it does not

address cell-specific alterations in the DNA methylation profile.(19) We used bead array technology for methylome profiling and were restricted to genomic sites that were included in the platform inferring a selection bias. Epigenetic modifications other than DNA methylation such as histone modifications, which may have an impact on transcriptional dysregulation in HF, were not assessed in this study.

In conclusion, heart failure is associated with common and distinct alterations in DNA methylation in ischemic versus non-ischemic failing myocardium. Mechanical unloading with LVAD fails to normalize the majority of HF-related DNA methylation, which remain persistently dysregulated. Differential DNA methylation regulates expression of both protein-coding and non-coding transcripts in the failing human heart with previously uncharacterized functions. Among these, *LINC00881* is a cardiac super-enhancer lncRNA, which is an essential regulator of cardiomyocyte calcium cycling. These findings suggest that epigenetic targeted therapies could be necessary to normalize the dysregulated transcriptome in the failing human myocardium and help achieve sustained clinical recovery from heart failure.

Methods

Study Subjects

Myocardial DNA methylation profiling was performed 36 patients with end-stage heart failure (12 Ischemic [ICM] and 24 Non-Ischemic [NICM] dilated cardiomyopathy, n=36 pre-LVAD) who underwent LVAD implantation at Columbia University Irving Medical Center including 8 patients with paired cardiac tissue at the time of heart transplantation (n= 8 post-LVAD) and non-failing control cardiac tissue (n=7, non-failing deceased donors) obtained from the National Disease Research Interchange (NDRI) in Philadelphia, PA, USA.

Genome-wide DNA Methylation Profiling

Left ventricular (LV) apical myocardial tissue samples were washed in ice-cold saline (0.9% NaCl) and stored in liquid nitrogen until DNA and RNA were extracted. DNA was extracted using a DNA Kit (Qiagen). Purity and concentration were determined using a Bioanalyzer (Agilent Technologies, CA). For DNA methylation profiling, DNA was bisulfite converted using a commercially available kit (Zymo Research, Orange, CA). Illumina Infinium Human Methylation 450K Bead Chip and EPIC Bead Chip were used for genome-wide profiling of DNA methylation.(58) The EPIC chip measures over 850 000 methylation sites, with high reproducibility in comparison to the previous 450k chip.(59) After whole genome DNA amplification, the samples were applied following the Illumina Infinium Human Methylation DNA chip manufacturer protocols (Illumina, San Diego, CA). Chips were analyzed using the Illumina Hi-Scan system at the McDonnell Genome Institute (MGI) at Washington University.

Bioinformatics Analysis

Integrated analysis of the 450K and EPIC Bead Array data was conducted using Bioconductor package ChAMP in R.(60) The analysis pipeline has been summarized in **Fig. S1**. Briefly, raw methylation data was imported into R and normalized using BMIQ. 450K and EPIC data was merged on common probes and corrected for batch effects using combat function. Additional filtering was performed for common SNPs. Differentially methylated positions (DMP) were identified using a cut-off of 10% change in methylation and q value <0.05. The first analysis focused on HF etiology and identified DMPs associated with ICM (ICM vs. NF) and NICM (NICM vs. NF) using data from pre-LVAD tissue obtained from 36 patients and 7 non-failing controls. The second analysis focused on the impact of mechanical unloading and identified DMPs that are associated with HF (pre-LVAD vs. NF) and reverse remodeling (post-LVAD vs. pre-LVAD) in 8 paired cardiac tissue samples. The variance in global DNA methylation between

subjects was assessed using principal component analysis (PCA) plots using the first three principal components. Hierarchical clustering of subjects was performed using the complete linkage method. DMPs common to ICM and NICM were screened for reciprocal changes in gene expression. RNA-sequencing data from left ventricular samples of 50 heart failure patients (13 with Ischemic and 37 with Non-Ischemic cardiomyopathy) and 14 non-failing controls was obtained from GEO (Accession number: 116250) and analyzed using the limma package in R. 36,755 transcripts with RPKM level of 0 in more than 50% of patients were filtered out. Data was log transformed using (RPKM + 1). Differential expression analysis was performed using linear model ANOVA. Differentially expressed genes (DEGs) were defined as genes with a p-value adjusted for Benjamini-Hochberg false discovery rate (FDR) ≤ 0.05 between heart failure and control samples. The locations of human cardiac super-enhancers were acquired from previous publications.(61, 62) ChIP-seq data is available through the Gene Expression Omnibus (GEO) using the following accession numbers: adult human heart H3K27ac (GSE101345), adult human heart H3K4me1 (GSE101156), adult human heart H3K27me3 (GSE101387), adult human heart CTCF (GSE 127553). DMPs located within intergenic regions were mapped to lnc-RNAs using GENCODE annotation database.(63) LINC00881 protein interactions were retrieved from the RNAct database using the catRAPID algorithm.(64)

Histopathological Examination of Human Heart Samples

Cardiomyocyte hypertrophy was determined by measuring cross-sectional area (CSA) of cardiomyocytes in H&E-stained paraffin embedded sections of human heart tissue. CSA of more than 100 cardiomyocytes with a centrally located nuclear was measured and averaged in each sample. The extent of myocardial fibrosis was determined by the percent area of Masson's

trichrome staining using random images obtained in each heart tissue section. Large epicardial vessels as well as cutting or compression artifacts were excluded from the analysis.

Cell Culture and Human Cardiomyocyte Differentiation

Induced pluripotent stem cells were obtained through material transfer agreements with Dr. Vunjak-Novakovic from B. Conklin, Gladstone Institute (WTC-11, healthy). Cells were maintained on 1:20 diluted growth factor reduced Matrigel (Corning, Corning, NY) in mTeSR-plus medium (StemCell Technologies, Vancouver, CA) supplemented with 1% penicillin/streptomycin (ThermoFisher Scientific, Waltham, MA) at 37°C, 21% O_2. iPS cells were passaged at 30–50% confluence using 0.5 mM EDTA (ThermoFisher Scientific, Waltham, MA) and cultured for 24 hours in iPS media supplemented with 5 μM Y-27632 (Tocris Biosciences, Bristol, UK) prior to maintenance in iPS media. Cells were used between passages 40 and 70.

Cardiac differentiation of human iPS cells was performed using a stage-based protocol in RPMI-1640 (ThermoFisher Scientific, Waltham, MA) supplemented with 0.5 mg/mL recombinant human albumin (Sigma-Aldrich, St. Louis, MO), 213 μg/mL L-ascorbic acid 2-phosphate (Sigma-Aldrich, St. Louis, MO), and 1% penicillin/streptomycin (CM media). iPS cells were grown to 80–90% confluence and changed into CM Media supplemented with 3 μM CHIR99021 (Tocris Biosciences, Bristol, UK) for 2 days. Media was then changed to CM Media supplemented with 2 μM Wnt-C59 (Tocris Biosciences, Bristol, UK) for 2 days prior to switching to CM Media without any supplements. CM Media is changed every 48 hours until contracting cells were noted by around day 10 following the initiation of differentiation, at which time the medium was changed to RPMI 1640 supplemented with B27 (50X; Gibco). Experiments were performed using hiPSC-CMs at day 15 – 35.

Flow Cytometry

Cells were dissociated using 500 µl TrypLE for 20 min at 37 °C and after a quick wash with PBS. Cells were collected by spinning down at 400 g for 3 min at RT. Cell pellet was resuspended in 4% fixative solution for 15 min at 4 °C and then treated in 0.1% Triton PBS buffer for 10 min at 4 °C. Cold PBS wash steps were performed. Cells were incubated 4 hours at 4 °C in the dark with *TNNT2* antibody at 1:500 (Santa Cruz, sc-20025). Cells were washed three times by cold PBS and centrifuged at 400 g for 3 min at room temperature. Cell pellet was resuspended in 500 µl of Alexa Fluro labelled secondary antibody at 1:1000 (Thermofisher, A21203) and incubated 2 hours at 4 °C in the dark. At least 10,000 events were analyzed for each sample in FACSCanto and data were analyzed and presented using FlowJo software. ≈85% of differentiated hiPSC-CMs stained positive for cardiac troponin T at day 22. (**Supplemental Figure 6**).

***LINC00881* Overexpression and Knockdown in Human iPS cell derived Cardiomyocytes**

Beating hiPSC-CMs were switched to Opti-MEM™ Reduced Serum Medium (ThermoFisher Scientific, Waltham, MA). *LINC000881* knockdown was achieved by lipofectamine based transfection of antisense LNA GapmeRs designed against *LINC00881* versus scrambled oligonucleotide (QIAGEN, Germantown, MD) using RNAiMAX reagent (ThermoFisher Scientific, Waltham, MA) (**Supplemental Table 13**). hiPSC-CMs were harvested at 48-72 hours following transfection for functional and gene expression studies. Knockdown of *LINC00881* was confirmed by qPCR. For *LINC00881* overexpression experiment, full length human LINC00881 was cloned into p3XFLAG-CMV-7 (Millipore Sigma, St. Louis, MO, USA) vector and amplified in DH5α strain of *Escherichia coli* (*E coli*) (Life Technologies, Grand Island NY). After amplification, plasmids were extracted through QIAGEN Plasmid Midi Kit (QIAGEN, Germantown, MD) and stored at −80 °C until use. Beating hiPSC-CMs were switched to Opti-MEM™ Reduced Serum Medium (ThermoFisher Scientific, Waltham, MA). *LINC000881*

overexpression was achieved by lipofectamine based transfection of *LINC00881* plasmid versus bacterial alkaline phosphatase control plasmid using RNAiMAX reagent (ThermoFisher Scientific, Waltham, MA). hiPSC-CMs were harvested at 48-72 hours following transfection for functional and gene expression studies. Overexpression of *LINC00881* was confirmed by qPCR.

Quantitative Real-time PCR

Total RNA was isolated from LV apical myocardial tissue and from beating hiPSC-CMs using Quick- RNA Miniprep Plus (Zymo Research, Irvine, CA, USA). The qRT-PCR was performed using SYBR mix (Thermofisher) on PicoReal96 Real-time PCR Systems (Thermoscintific). Transcript quantification for mRNAs were performed using delta-delta method using forward and reverse primers designed specifically for each of the target mRNAs and lncRNAs. The primer sequences used for independent validation are listed in **Supplemental Table 13**. 18S was used as internal control.

RNA sequencing and Data Analysis

RNA concentration and integrity were assessed using a 2100 BioAnalyzer (Agilent, Santa Clara CA). Sequencing libraries were constructed using the TruSeq Stranded Total RNA Library Prep Gold mRNA (Illumina, San Diego CA) with an input of 1000 ng and 11 cycles final amplification. Final libraries were quantified using High Sensitivity D1000 ScreenTape on a 2200 TapeStation (Agilent, Santa Clara CA) and Qubit 1x dsDNA HS Assay Kit (Invitrogen, Waltham MA). Samples were pooled equimolar with sequencing performed on an Illumina NovaSeq6000 SP 300 Cycle Flow Cell v1.5 as Paired-end 151 reads. Sequences from fastq files were aligned to reference human genome (Gencode v38) using the splice-aware aligner STAR v.2.7.3a. Differential gene expression analysis with *LINC00881* knockdown or overexpression was performed using the R package DESeq2 (v1.34.0) from unnormalized count data.

Human iPS Cell derived Cardiomyocyte Calcium Imaging

Human iPS cell derived cardiomyocyte monolayers were loaded with 5μM Calbryte-590 in RPMI + B27 medium at 37ºC for 45 minutes. Loading media was washed and replaced with Tyrode's salt solution. Calcium transience videos were acquired at 50 frames per second using a sCMOS camera (Zyla 4.2, Andor Technology) connected to an inverted fluorescence microscope (IX-81, Olympus) with cells placed in a live-cell chamber (STX Temp & CO_2 Stage Top Incubator, Tokai Hit). Calcium signal analysis was performed using custom Python script as previously described.(65)

RNA Immunoprecipitation

The immunoprecipitation assay was performed in 2 million hiPSC-CMs. Cells were crosslinked with 1% formaldehyde in PBS for 10 min at 37 °C and quenched with 1.25M glycine. Cells were suspended in 1 ml of RIPA buffer (50 mM Tris, pH 7.4, 150 mM NaCl, 1 mM EDTA, 0.1% SDS, 1% NP-40, and 0.5% sodium deoxycholate, 0.5mM DTT, 100 U/ml RNAseOUT, and 1X protease inhibitor cocktail), and incubated on ice for 30 minutes followed by centrifugation at 13,000 RPM for 10 min. Lysates were pre-cleared with washed Protein A/G magnetic beads (Thermofisher) at 4°C for 30 minutes. 30 μl Protein A/G magnetic beads (Thermofisher) were incubated with 5 μg *SMARCA4* antibody (Proteintech, 31634-1-AP) or IgG control (Proteintech, 30000-0-AP) in 200 μl RIPA buffer for 30 min at room temperature followed by incubation with pre-cleared lysate for 4 hours at 4ºC. Samples were washed two times in RIPA buffer, four times in 1M high salt RIPA buffer (50 mM Tris, pH 7.4, 1 M NaCl, 1 mM EDTA, 0.1% SDS, 1% NP-40, and 0.5% sodium deoxycholate), and then twice in RIPA. RNA samples were extracted with Trizol.

Chromatin Accessibility Assay

Chromatin accessibility was performed using the EpiQuik™ Chromatin Accessibility Assay Kit (Epigentek). Briefly, hiPSC-CMs with or without *LINC00881* overexpression were lysed and chromatin was isolated. One chromatin aliquot was digested with nuclease, while the other was untreated. After incubation at 37 C for 4 minutes, reaching was quenched by adding stop solution. DNA was isolated followed by qPCR to amplify DNA for *MYH6, CACNA1C, and RYR2* gene promoters. Primer sequences used for chromatin accessibility are listed in **Supplemental Table 13**. Fold enrichment was calculated using formula: $FE = 2^{(Ct\ level\ with\ nuclease - Ct\ level\ without\ nuclease)}$.

Data Sharing

Genome-wide DNA methylation data from human heart failure (GSE197670) and RNA sequencing data from human iPS cell derived cardiomyocytes (GSE197671) are available in NCBI's Gene Expression Omnibus (GEO).

Statistics

Statistical analyses were performed using R (R Core Team, 2021). Continuous data are presented as mean ± standard error of the mean. For comparisons between two groups, a two tailed unpaired t-test was used. For comparisons between three or more groups, one-way ANOVA with Fisher's post hoc test or Kruskal-Wallis with Wilcoxon post hoc were used. p value less than 0.05 was considered statistically significant in all analyses.

Study Approval

The study was approved by Columbia University Irving Medical Center Institutional Review Board (IRB#AAAR0055). Written informed consent was obtained for the procurement of discarded LV apical myocardial tissue at the time of LVAD implantation and cardiac transplantation.

Author Contributions

X.L. performed majority of experiments with help from P.J.K., B.L., T.R.N, R.Z.Z., A.G.F., C.X., and R.L. V.K.T. and X.L. designed the experiments. V.K.T., X.L., and P.J.K. wrote the manuscript with input from co-authors. P.C.C., N.U., S.O.M., M.P.R, and G.V.N. provided conceptual advice. V.K.T. coordinated and oversaw the whole project. X.L. was listed first because he performed majority of experiments.

Acknowledgements

Authors thank Dr. Benjamin Tycko and Dr. Catherine Do from Columbia University Epigenetics Core for their assistance with DNA methylation data analysis. Graphical abstract was created with Biorender.com.

Conflict of Interest

P.C.C. reported receiving professional fees from Roche and Abbott. N.U. reported receiving grants from Abbott, Abiomed, and Fire 1 and serving on a medical advisory board Livemetric, Leviticus, and Revamp outside the submitted work.

Material Availability: All unique reagents generated in this study are available from the lead contact with a completed materials transfer agreement

References

1. Virani SS, et al. Heart Disease and Stroke Statistics-2020 Update: A Report From the American Heart Association. *Circulation.* 2020;141(9):e139-e596.
2. Hartupee J, and Mann DL. Neurohormonal activation in heart failure with reduced ejection fraction. *Nat Rev Cardiol.* 2017;14(1):30-8.
3. Taegtmeyer H, et al. Return to the fetal gene program: a suggested metabolic link to gene expression in the heart. *Ann N Y Acad Sci.* 2010;1188:191-8.
4. Barth AS, et al. Reciprocal transcriptional regulation of metabolic and signaling pathways correlates with disease severity in heart failure. *Circ Cardiovasc Genet.* 2011;4(5):475-83.
5. Sweet ME, et al. Transcriptome analysis of human heart failure reveals dysregulated cell adhesion in dilated cardiomyopathy and activated immune pathways in ischemic heart failure. *BMC Genomics.* 2018;19(1):812.
6. Kittleson MM, et al. Identification of a gene expression profile that differentiates between ischemic and nonischemic cardiomyopathy. *Circulation.* 2004;110(22):3444-51.
7. Margulies KB, et al. Mixed messages: transcription patterns in failing and recovering human myocardium. *Circ Res.* 2005;96(5):592-9.
8. Yang KC, et al. Deep RNA sequencing reveals dynamic regulation of myocardial noncoding RNAs in failing human heart and remodeling with mechanical circulatory support. *Circulation.* 2014;129(9):1009-21.
9. Topkara VK, et al. Functional significance of the discordance between transcriptional profile and left ventricular structure/function during reverse remodeling. *JCI Insight.* 2016;1(4):e86038.
10. Akazawa H, and Komuro I. Roles of cardiac transcription factors in cardiac hypertrophy. *Circ Res.* 2003;92(10):1079-88.
11. Kim SY, et al. Epigenetic regulation in heart failure. *Curr Opin Cardiol.* 2016;31(3):255-65.
12. Moore LD, et al. DNA methylation and its basic function. *Neuropsychopharmacology.* 2013;38(1):23-38.
13. Ehrlich M. DNA hypomethylation in cancer cells. *Epigenomics.* 2009;1(2):239-59.
14. Song L, et al. The performance of the SEPT9 gene methylation assay and a comparison with other CRC screening tests: A meta-analysis. *Sci Rep.* 2017;7(1):3032.
15. Hao X, et al. DNA methylation markers for diagnosis and prognosis of common cancers. *Proc Natl Acad Sci U S A.* 2017;114(28):7414-9.
16. Garcia-Manero G. Demethylating agents in myeloid malignancies. *Curr Opin Oncol.* 2008;20(6):705-10.
17. Movassagh M, et al. Distinct epigenomic features in end-stage failing human hearts. *Circulation.* 2011;124(22):2411-22.
18. Haas J, et al. Alterations in cardiac DNA methylation in human dilated cardiomyopathy. *EMBO Mol Med.* 2013;5(3):413-29.
19. Gilsbach R, et al. Dynamic DNA methylation orchestrates cardiomyocyte development, maturation and disease. *Nat Commun.* 2014;5:5288.
20. Glezeva N, et al. Targeted DNA Methylation Profiling of Human Cardiac Tissue Reveals Novel Epigenetic Traits and Gene Deregulation Across Different Heart Failure Patient Subtypes. *Circ Heart Fail.* 2019;12(3):e005765.

21. Pepin ME, et al. DNA methylation reprograms cardiac metabolic gene expression in end-stage human heart failure. *Am J Physiol Heart Circ Physiol.* 2019;317(4):H674-H84.
22. Koczor CA, et al. Detection of differentially methylated gene promoters in failing and nonfailing human left ventricle myocardium using computation analysis. *Physiol Genomics.* 2013;45(14):597-605.
23. Meder B, et al. Epigenome-Wide Association Study Identifies Cardiac Gene Patterning and a Novel Class of Biomarkers for Heart Failure. *Circulation.* 2017;136(16):1528-44.
24. Varley KE, et al. Dynamic DNA methylation across diverse human cell lines and tissues. *Genome Res.* 2013;23(3):555-67.
25. Luo C, et al. Dynamic DNA methylation: In the right place at the right time. *Science.* 2018;361(6409):1336-40.
26. Spainhour JC, et al. Correlation Patterns Between DNA Methylation and Gene Expression in The Cancer Genome Atlas. *Cancer Inform.* 2019;18:1176935119828776.
27. Movassagh M, et al. Differential DNA methylation correlates with differential expression of angiogenic factors in human heart failure. *PLoS One.* 2010;5(1):e8564.
28. Pepin ME, et al. Genome-wide DNA methylation encodes cardiac transcriptional reprogramming in human ischemic heart failure. *Lab Invest.* 2019;99(3):371-86.
29. Ito E, et al. Histone Modification Is Correlated With Reverse Left Ventricular Remodeling in Nonischemic Dilated Cardiomyopathy. *Ann Thorac Surg.* 2017;104(5):1531-9.
30. Mann DL, et al. Myocardial recovery and the failing heart: myth, magic, or molecular target? *J Am Coll Cardiol.* 2012;60(24):2465-72.
31. Birks EJ. Molecular changes after left ventricular assist device support for heart failure. *Circ Res.* 2013;113(6):777-91.
32. Topkara VK, et al. Myocardial Recovery in Patients Receiving Contemporary Left Ventricular Assist Devices: Results From the Interagency Registry for Mechanically Assisted Circulatory Support (INTERMACS). *Circ Heart Fail.* 2016;9(7).
33. Burkhoff D, et al. Reverse Remodeling With Left Ventricular Assist Devices. *Circ Res.* 2021;128(10):1594-612.
34. Xiao D, et al. Inhibition of DNA methylation reverses norepinephrine-induced cardiac hypertrophy in rats. *Cardiovasc Res.* 2014;101(3):373-82.
35. Vujic A, et al. Experimental heart failure modelled by the cardiomyocyte-specific loss of an epigenome modifier, DNMT3B. *J Mol Cell Cardiol.* 2015;82:174-83.
36. Chen H, et al. DNA Methylation Indicates Susceptibility to Isoproterenol-Induced Cardiac Pathology and Is Associated With Chromatin States. *Circ Res.* 2016;118(5):786-97.
37. Zhou J, et al. Weighted correlation network bioinformatics uncovers a key molecular biosignature driving the left-sided heart failure. *BMC Med Genomics.* 2020;13(1):93.
38. Colak D, et al. Left ventricular global transcriptional profiling in human end-stage dilated cardiomyopathy. *Genomics.* 2009;94(1):20-31.
39. Zhou LY, et al. The circular RNA ACR attenuates myocardial ischemia/reperfusion injury by suppressing autophagy via modulation of the Pink1/ FAM65B pathway. *Cell Death Differ.* 2019;26(7):1299-315.
40. Franaszczyk M, et al. Analysis of De Novo Mutations in Sporadic Cardiomyopathies Emphasizes Their Clinical Relevance and Points to Novel Candidate Genes. *J Clin Med.* 2020;9(2).

41. Molina-Navarro MM, et al. Heart failure entails significant changes in human nucleocytoplasmic transport gene expression. *Int J Cardiol.* 2013;168(3):2837-43.
42. Taglieri DM, et al. The C-terminus of the long AKAP13 isoform (AKAP-Lbc) is critical for development of compensatory cardiac hypertrophy. *J Mol Cell Cardiol.* 2014;66:27-40.
43. Shende P, et al. Cardiac raptor ablation impairs adaptive hypertrophy, alters metabolic gene expression, and causes heart failure in mice. *Circulation.* 2011;123(10):1073-82.
44. Zhang CL, et al. Class II histone deacetylases act as signal-responsive repressors of cardiac hypertrophy. *Cell.* 2002;110(4):479-88.
45. Thum T, et al. MicroRNA-21 contributes to myocardial disease by stimulating MAP kinase signalling in fibroblasts. *Nature.* 2008;456(7224):980-4.
46. Hinkel R, et al. AntimiR-21 Prevents Myocardial Dysfunction in a Pig Model of Ischemia/Reperfusion Injury. *J Am Coll Cardiol.* 2020;75(15):1788-800.
47. Sano M, et al. Genome-Wide Association Study of Absolute QRS Voltage Identifies Common Variants of TBX3 as Genetic Determinants of Left Ventricular Mass in a Healthy Japanese Population. *PLoS One.* 2016;11(5):e0155550.
48. Li Y, et al. Comparative transcriptomic analysis of multiple cardiovascular fates from embryonic stem cells predicts novel regulators in human cardiogenesis. *Sci Rep.* 2015;5:9758.
49. Ang YS, et al. Disease Model of GATA4 Mutation Reveals Transcription Factor Cooperativity in Human Cardiogenesis. *Cell.* 2016;167(7):1734-49 e22.
50. Thum T, et al. MicroRNAs in the human heart: a clue to fetal gene reprogramming in heart failure. *Circulation.* 2007;116(3):258-67.
51. Xiao C, et al. Chromatin-remodelling factor Brg1 regulates myocardial proliferation and regeneration in zebrafish. *Nat Commun.* 2016;7:13787.
52. Alexander JM, et al. Brg1 modulates enhancer activation in mesoderm lineage commitment. *Development.* 2015;142(8):1418-30.
53. Hang CT, et al. Chromatin regulation by Brg1 underlies heart muscle development and disease. *Nature.* 2010;466(7302):62-7.
54. Li YM, et al. Replication-Independent Histone Turnover Underlines the Epigenetic Homeostasis in Adult Heart. *Circulation Research.* 2019;125(2):198-208.
55. Willis MS, et al. BRG1 and BRM function antagonistically with c-MYC in adult cardiomyocytes to regulate conduction and contractility. *Journal of Molecular and Cellular Cardiology.* 2017;105:99-109.
56. Wang L, et al. Single-cell reconstruction of the adult human heart during heart failure and recovery reveals the cellular landscape underlying cardiac function. *Nat Cell Biol.* 2020;22(1):108-+.
57. Alimadadi A, et al. Meta-Analysis of Dilated Cardiomyopathy Using Cardiac RNA-Seq Transcriptomic Datasets. *Genes (Basel).* 2020;11(1).
58. Dedeurwaerder S, et al. Evaluation of the Infinium Methylation 450K technology. *Epigenomics.* 2011;3(6):771-84.
59. Logue MW, et al. The correlation of methylation levels measured using Illumina 450K and EPIC BeadChips in blood samples. *Epigenomics.* 2017;9(11):1363-71.
60. Tian Y, et al. ChAMP: updated methylation analysis pipeline for Illumina BeadChips. *Bioinformatics.* 2017;33(24):3982-4.

61. Hnisz D, et al. Super-enhancers in the control of cell identity and disease. *Cell.* 2013;155(4):934-47.
62. Khan A, and Zhang X. dbSUPER: a database of super-enhancers in mouse and human genome. *Nucleic Acids Res.* 2016;44(D1):D164-71.
63. Frankish A, et al. GENCODE reference annotation for the human and mouse genomes. *Nucleic Acids Res.* 2019;47(D1):D766-D73.
64. Lang B, et al. RNAct: Protein-RNA interaction predictions for model organisms with supporting experimental data. *Nucleic Acids Res.* 2019;47(D1):D601-D6.
65. Tamargo MA, et al. milliPillar: A Platform for the Generation and Real-Time Assessment of Human Engineered Cardiac Tissues. *ACS Biomater Sci Eng.* 2021;7(11):5215-29.

Table 1. Clinical Characteristics of Study Subjects with Genome-wide DNA Methylation Profiling at the time of LVAD implantation

Variables	Full Cohort (n=36)	Ischemic HF (n=12)	Non-Ischemic HF (n=24)	p-value
Age	56.7 ± 13.3	64.7 ± 6.4	52.65 ± 14.2	**0.008**
Gender (M)	69% (25)	67% (8)	71% (17)	0.999
Ethnicity				
White	53% (19)	83% (10)	38% (9)	**0.014**
African American	36% (13)	8% (1)	50% (12)	**0.025**
Asian	2% (1)	0% (0)	4% (1)	0.999
Hispanic	8% (3)	8% (1)	8% (2)	0.999
LVAD Type				
Heartmate II	83% (30)	58% (7)	96% (23)	**0.010**
Heartware HVAD	17% (6)	42% (5)	4% (1)	
Destination Therapy	44% (16)	42% (5)	46% (11)	0.999
LVEF (%)	15 ± 4	17 ± 3	14 ± 3	**0.023**
LVEDD (cm)	7.1 ± 1	6.7 ± 1.1	7.3 ± 1	0.121
Serum Creatinine (mg/dL)	1.41 ± 0.58	1.26 ± 0.32	1.49 ± 0.67	0.283
Serum BNP (ng/L)	1402 ± 1564	1061 ± 918	1597 ± 1828	0.353
Medication Use				
Beta-blocker	83% (30)	92% (11)	79% (19)	0.640
RAAS inhibitors	64% (23)	58% (7)	67% (16)	0.720
Diuretics	47% (17)	58% (7)	42% (10)	0.483
Antiarrhythmics	53% (19)	58% (7)	50% (12)	0.732
Duration of support (days)	627 ± 487	652 ± 522	577 ± 424	0.672
LVAD Outcome				
Death	22% (8)	33% (4)	17% (4)	0.397
Transplant	61% (22)	50% (6)	67% (16)	0.472
Ongoing	8% (3)	0% (0)	13% (3)	0.536
Transferred care	8% (3)	17% (2)	4% (1)	0.253

Table 2. DNA Methylation vs. mRNA Expression Correlation of Differentially Methylated Positions Common to ICM and NICM

DNAm	mRNA	Gene	Log FC	AveExpr	t	P value	Adj. p	B	Delta B
Hypo-methylated	Up-regulated	HTRA1	1.014	6.316	7.864	<0.001	<0.001	14.911	-0.132
		FAM65B	0.822	2.262	4.827	<0.001	<0.001	3.198	-0.161
		FBXO16	0.726	2.274	5.119	<0.001	<0.001	4.248	-0.122
		EFCAB13	0.483	1.259	3.059	0.003	0.010	-2.385	-0.198
		COL18A1	0.467	5.685	1.783	0.079	0.142	-5.207	-0.136
		UNC45A	0.460	4.032	5.407	<0.001	<0.001	5.305	-0.119
		KALRN	0.439	5.233	3.638	0.001	0.002	-0.732	-0.140
		AKAP13	0.430	7.326	4.383	<0.001	<0.001	1.659	-0.124
		RPTOR	0.419	3.359	4.728	<0.001	<0.001	2.849	-0.205
		KIAA0922	0.349	3.258	3.184	0.002	0.007	-2.045	-0.152
		HDAC9	0.347	3.486	2.322	0.023	0.052	-4.168	-0.140
		PLXNA2	0.345	3.962	2.960	0.004	0.013	-2.646	-0.174
		BRE	0.343	5.701	5.139	<0.001	<0.001	4.319	-0.156
		MAP3K14	0.261	3.396	2.397	0.019	0.045	-4.005	-0.138
	Down-regulated	PRDM16	-0.285	2.458	-2.704	0.009	0.023	-3.292	-0.133
		STXBP5	-0.286	2.405	-2.703	0.009	0.023	-3.294	-0.147
		BATF	-0.291	1.178	-1.255	0.214	0.316	-5.983	-0.121
		PLD6	-0.330	2.603	-2.744	0.008	0.021	-3.195	-0.141
		SYN2	-0.339	1.276	-1.494	0.140	0.225	-5.663	-0.133
		PDE4D	-0.352	3.379	-2.235	0.029	0.062	-4.352	-0.127
		ANKRD6	-0.372	3.635	-2.908	0.005	0.014	-2.781	-0.142
		FRK	-0.417	1.906	-3.230	0.002	0.007	-1.919	-0.106
		ABLIM1	-0.427	8.671	-5.452	<0.001	<0.001	5.474	-0.191
		SOD2	-0.578	9.177	-5.893	<0.001	<0.001	7.141	-0.118
		PARD3	-0.699	4.697	-7.768	<0.001	<0.001	14.526	-0.123
		PALLD	-0.998	8.631	-9.168	<0.001	<0.001	20.098	-0.162
		RARRES1	-1.755	4.029	-4.402	<0.001	<0.001	1.721	-0.149
Hyper-methylated	Up-regulated	PCDHGA2	0.740	2.127	6.295	<0.001	<0.001	8.695	0.148
		ATOH8	0.701	4.693	4.155	<0.001	0.001	0.897	0.109
		SOX9	0.617	3.453	3.977	<0.001	0.001	0.324	0.123
		CPT1C	0.495	2.080	3.135	0.003	0.008	-2.180	0.156
		RAB11FIP1	0.417	3.402	2.219	0.030	0.064	-4.386	0.122
		PRRT1	0.270	2.535	2.233	0.029	0.062	-4.355	0.108
	Down	TBX3	-0.537	3.790	-3.840	<0.001	0.001	-0.111	0.123

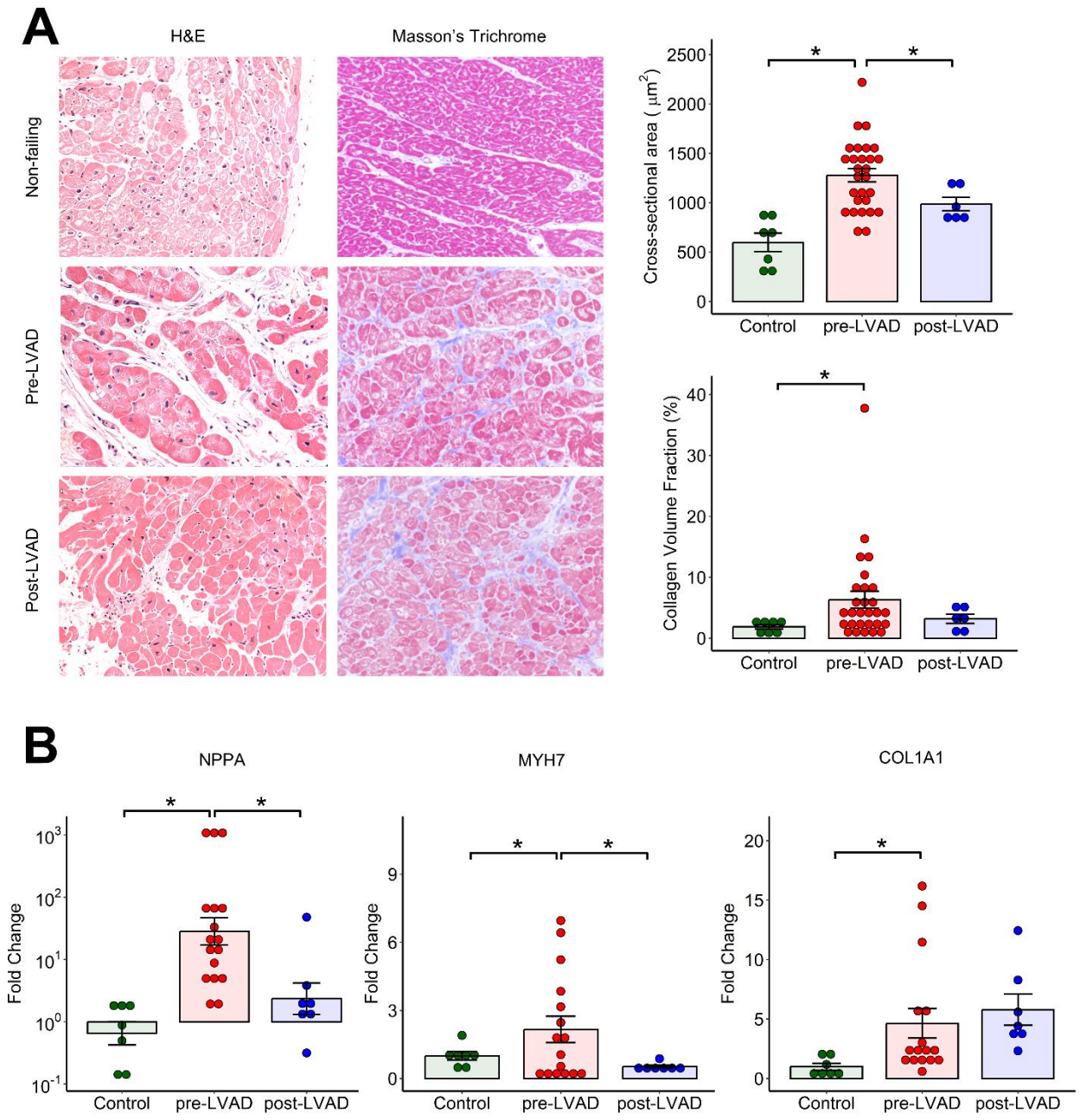

Figure 1. Impact of Mechanical Unloading on Histopathology and Gene Expression of the Failing Human Heart. **A)** Cardiomyocyte-cross sectional area (CSA) by H&E staining and myocardial collagen deposition by Masson's trichrome staining (* $p<0.05$, Kruskal Wallis test with pairwise BH-corrected Wilcoxon test, n=7 controls, 28 pre-LVAD, and 6 post-LVAD patients), 20x original magnification fields, **B)** Myocardial *NPPA*, *MYH7*, and *COL1A1* mRNA levels by RT-qPCR (* $p<0.05$, Kruskal Wallis test with pairwise BH-corrected Wilcoxon test, n=7 controls, 17 pre-LVAD, and 7 post-LVAD patients).

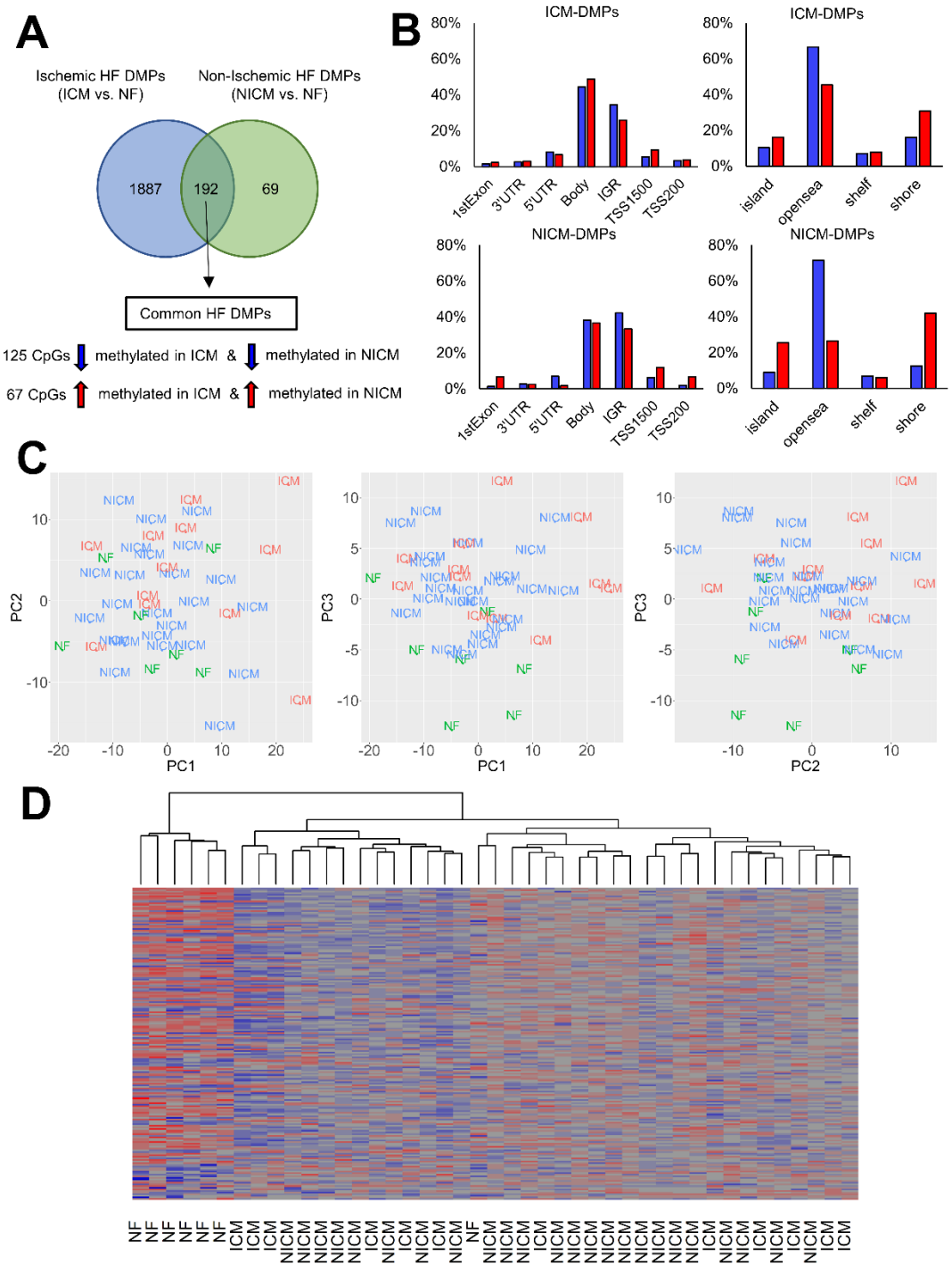

Figure 2. Genome-wide Changes in Myocardial DNA Methylation Based on HF Etiology. **A)** Venn diagram depicting the number of differentially methylated positions (DMPs) in patients with Ischemic (ICM) versus Non-ischemic cardiomyopathy (q<0.05, |Delta Beta| >10%), **B)** Proportion of ICM and NICM DMPs by genomic location and feature, **C)** Principal component analysis of myocardial DNA methylation grouped by etiology of HF (NF: non-failing [green], ICM: ischemic cardiomyopathy [red], and NICM: non-ischemic cardiomyopathy [blue]), **D)** Heatmap clustering of subjects by methylation profile of 192 Common HF DMPs.

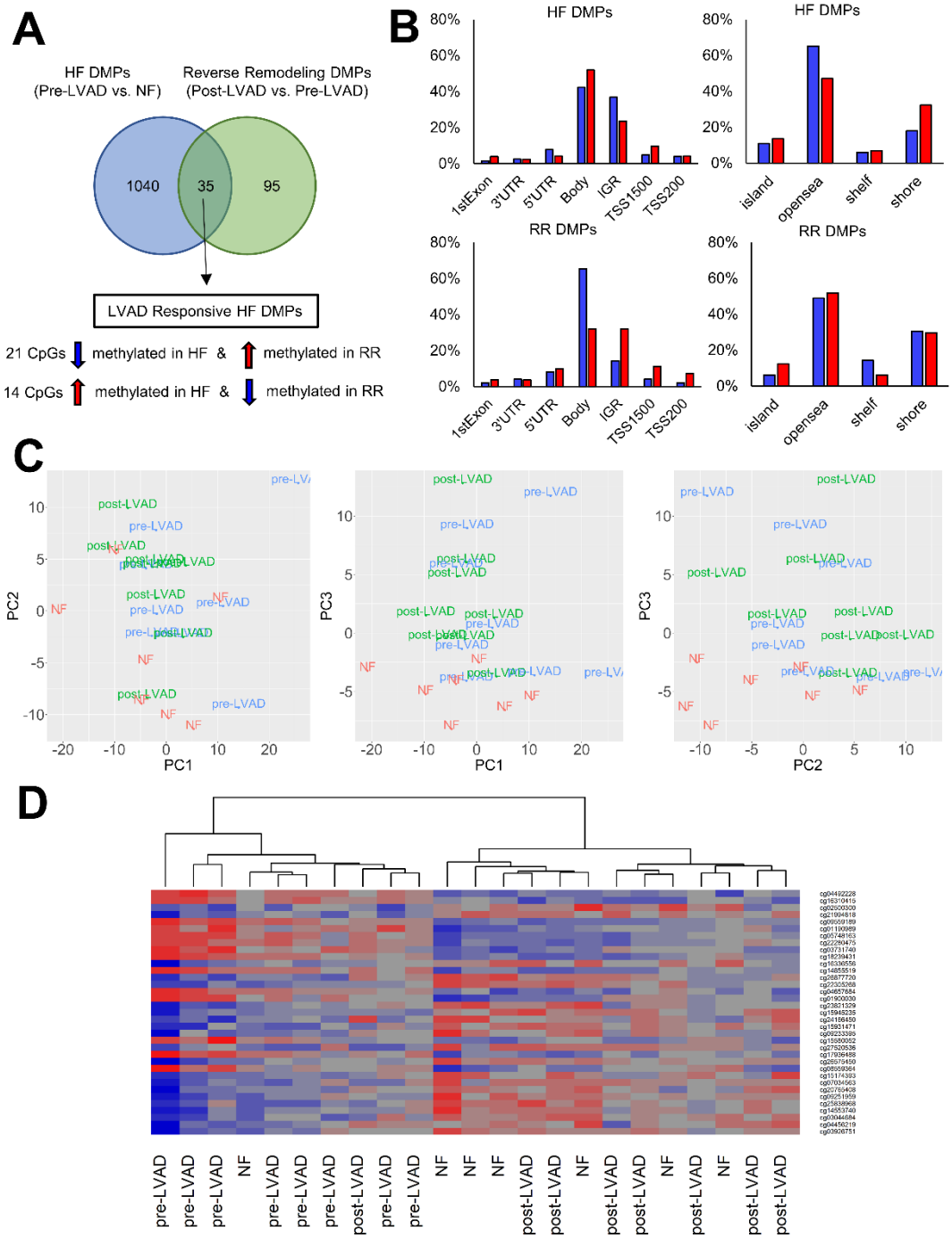

Figure 3. Impact of Mechanical Unloading on Myocardial DNA Methylation Profile. **A)** Venn diagram depicting the number of differentially methylated positions (DMPs) in Heart Failure (pre-LVAD vs. Non-Failing) versus Reverse Remodeling (post-LVAD vs. pre-LVAD) (q<0.05, |Delta Beta| >10%), **B)** Proportion of HF and reverse remodeling DMPs by genomic location and feature, **C)** Principal component analysis of myocardial DNA methylation before and after LVAD support (NF: non-failing [red], pre-LVAD [blue], and post-LVAD [green]), **D)** Heatmap clustering of subjects by 35 LVAD Responsive HF DMPs.

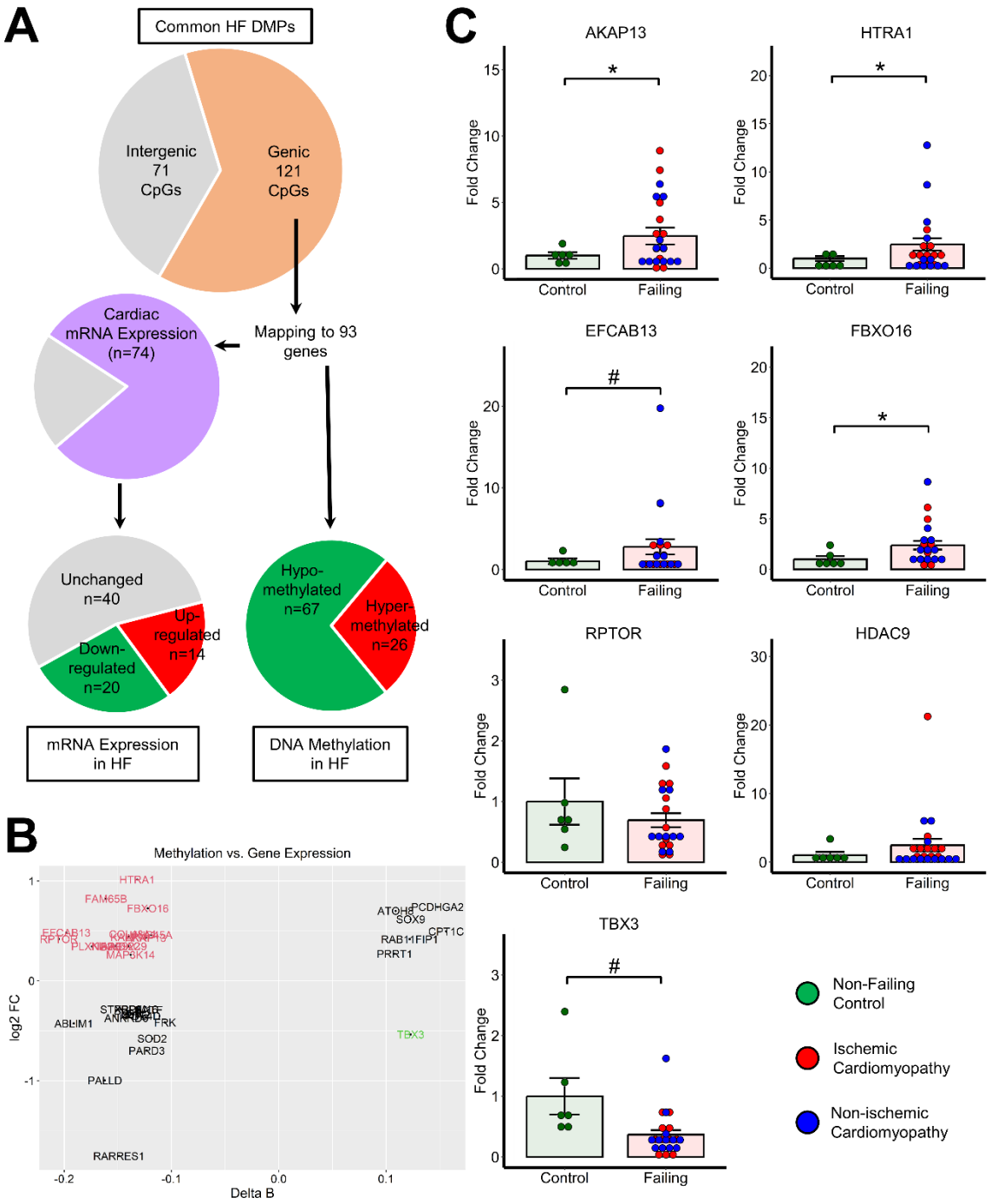

Figure 4. Correlation of DNA Methylation with Gene Expression in Human Heart Failure. **A)** Differential Methylation and Gene Expression of 192 Common Heart Failure DMPs, **B)** Methylation vs. Gene Expression Correlation Plot, **C)** qPCR validation of candidate genes that are epigenetically regulated in independent samples obtained from HF patients. * $p<0.05$, # $p<0.10$; unpaired t test; n= 6 (Control) and 23 (Failing). Data shown as mean ± SEM.

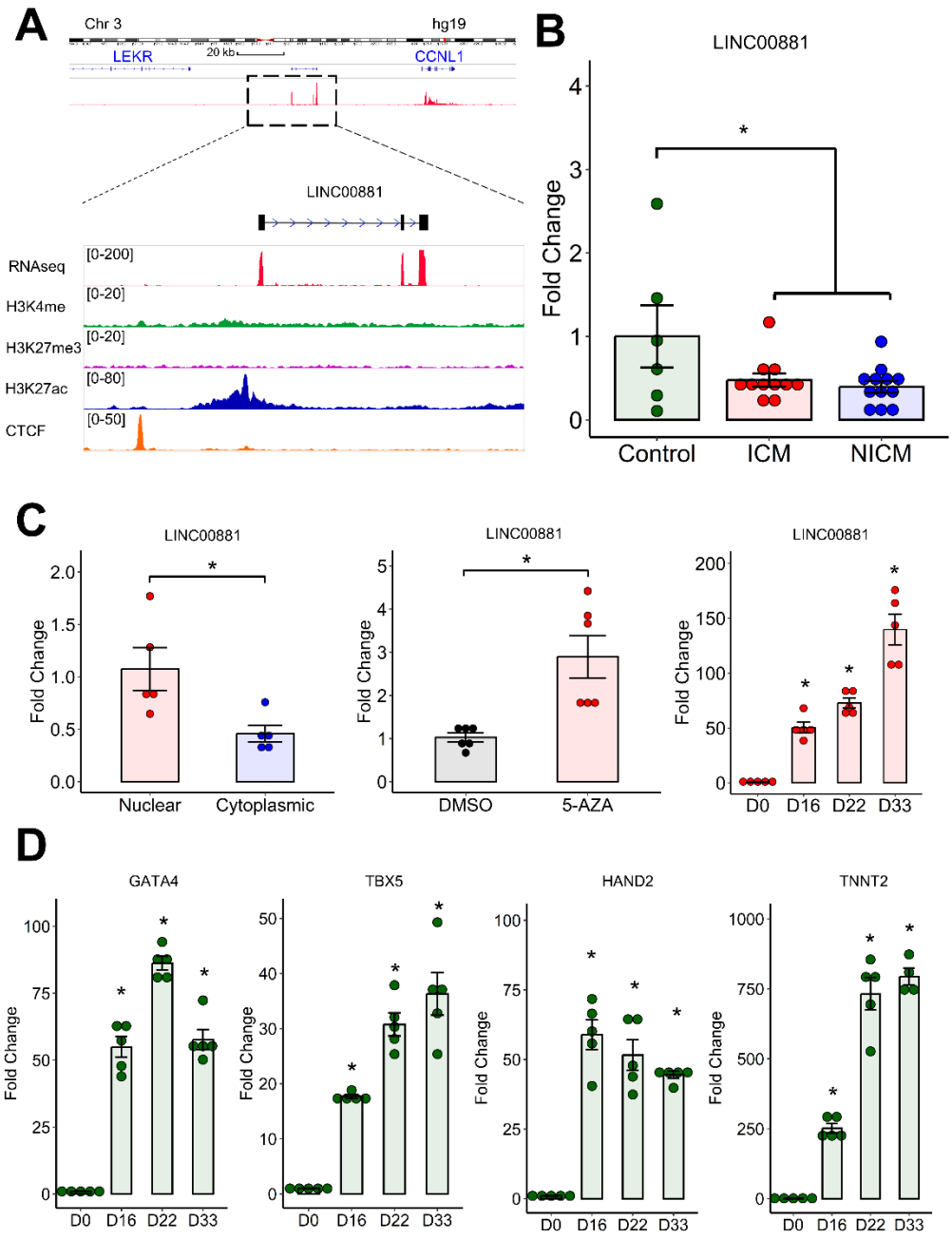

Figure 5. *LINC00881* is a cardiomyocyte lineage-specific super-enhancer lincRNA. **A)** Position, expression, and epigenetic regulation of the *LINC00881* locus in the non-failing human heart, **B)** Expression of *LINC00881* in patients with ischemic (ICM) and non-ischemic (NICM) cardiomyopathy by qPCR (* p<0.05, one-way ANOVA with Fisher's post-hoc; n=6 controls, 11 ICM, and 12 NICM), **C)** Expression of *LINC00881* in the nuclear versus cytoplasmic fractions (* p <0.05, unpaired t test, n= 6/group), with or without treatment with 20 nM 5-Azacytidine (5-AZA) (* p<0.05, unpaired t test, n=6/group), in hiPSC-CMs (* p<0.05, one-way ANOVA with Fisher's post hoc compared to Day 0, n=5/group), **D)** Expression levels of *LINC00881* and cardiac transcription factors during hiPSC-CM differentiation (* p<0.05, one-way ANOVA with Fisher's post-hoc compared to Day 0, n=5/group). Data shown as mean ± SEM.

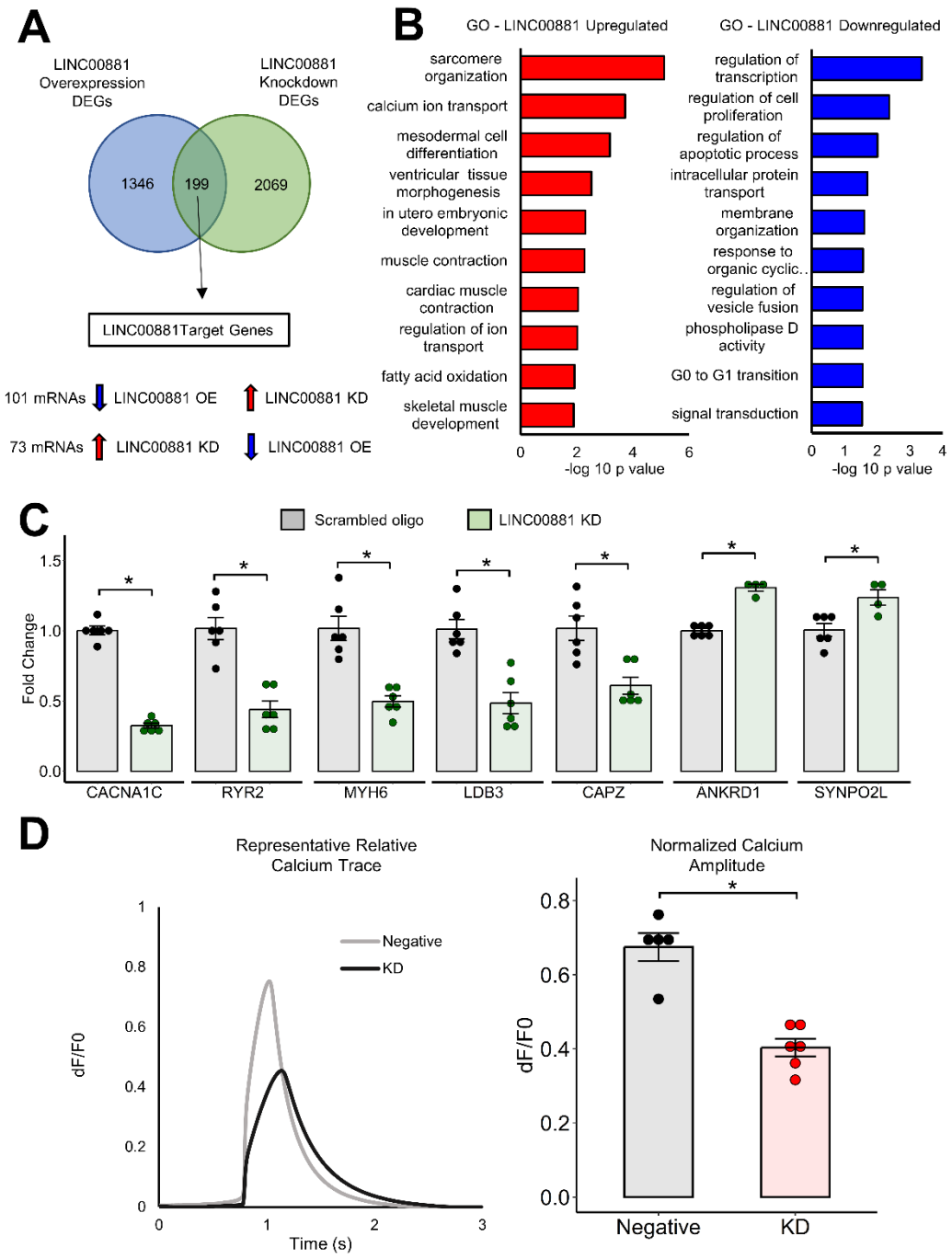

Figure 6. *LINC00881* is an essential regulator of cardiomyocyte calcium cycling. **A)** Venn-diagram depicting the number of differentially expressed genes in human iPS derived cardiomyocytes (hiPSC-CMs) with *LINC00881* plasmid-based overexpression or GapmeR-mediated knockdown, **B)** Gene Ontology analysis of gene targets that are positively or negatively regulated by *LINC00881* for Biological Process, **C)** qPCR validation of LINC00881 target genes (* $p<0.05$, unpaired t test, n=4-6/group), **D)** Representative relative calcium traces in beating hiPSC-CMs with *LINC00881* versus scrambled oligonucleotide knockdown with averaged normalized calcium amplitude (* $p<0.05$, unpaired t test, n=5-6/group). Data shown as mean ± SEM.

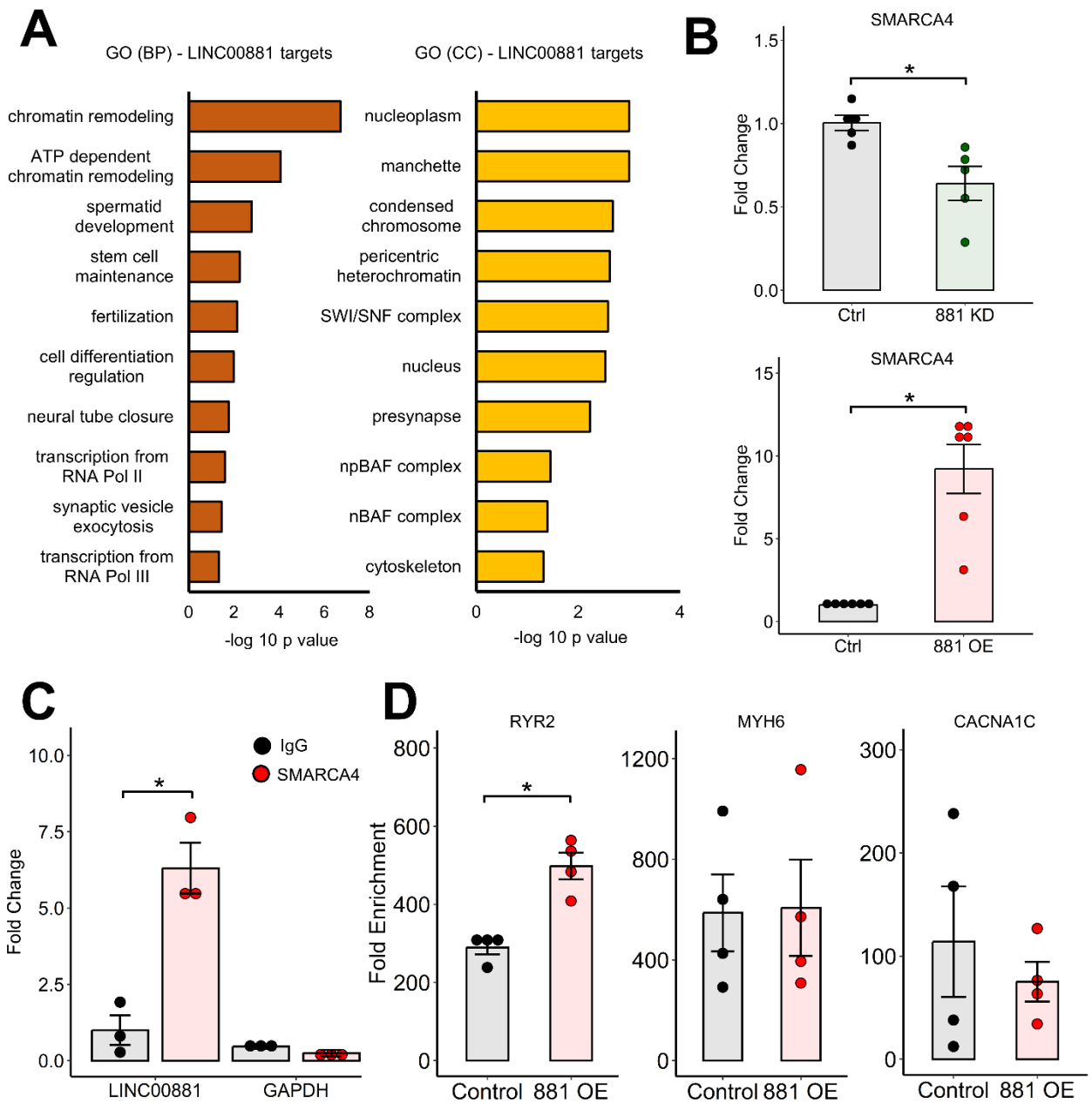

Figure 7. *LINC00881* regulates chromatin remodeling in human cardiomyocytes. **A)** Gene Ontology analysis of putative LINC00881 protein targets for Biological Process (BP) and Cellular Component (CC) sub-ontologies, **B)** *SMARCA4* mRNA levels with *LINC00881* knockdown or *LINC00881* overexpression in hiPSC-CMs by qPCR (* $p<0.05$, unpaired t test, n=5-6/group), **C)** RNA immunoprecipitation of *LINC00881* or *GAPDH* transcripts using *SMARCA4* antibody versus IgG control by qPCR in hiPSC-CMs (* $p<0.05$, unpaired t test, n=3/group, data representative of 3 experiments), **D)** Chromatin accessibility of *MYH6*, *RYR2*, and *CACNA1C* promoters with or without *LINC00881* overexpression in hiPSC-CMs by qPCR (* $p<0.05$, unpaired t test, n=4/group). Data shown as mean ± SEM.